Electronic Supplementary Material (ESI) for Materials Chemistry Frontiers.
This journal is © the Partner Organisations 2021

Supporting Information

Facile fabrication of $CuCo_2S_4$ nanoparticles/MXene composite as anode for high-performance asymmetric supercapacitor

Xiaobo Chen [a*], Zimin Ding[a], Huan Yu[a], Huiran Ge[a], Weiwei Liu[a], Shixin Sun[b*]

a School of Physics and Electronic Engineering, Yancheng Teachers University, Yancheng, 224051, PR China.

E-mail: chenxbok@126.com

b College of Chemical and Environmental Engineering, Yancheng Teachers University, Yancheng 224002, PR China.

E-mail: asunshixin@163.com

Experimental details

Structural characterizations

The X-ray diffraction (XRD) patterns recorded using a SHIMADZU XRD-6100 instrument with Cu-Kα radiation. The X-ray photoelectron spectra (XPS) were collected by a Thermo ESCALAB 250 electron spectrometer with an X-ray source of Al Ka. The scanning electron microscopy (SEM) imaging was conducted by Zeiss Supra 35VP scanning electron microscope, and the transmission electron microscopy (TEM) and high-resolution TEM (HRTEM) imaging was conducted by JEOL-2010 transmission electron microscope with 200 kV accelerated voltage. The specific surface area (BET method) of the samples were determined by nitrogen (N_2) adsorption/desorption using an ASAP 2020 V3.01 G instrument.

Electrochemical measurements

In this experiment, an active material (Ti_3C_2 MXene, $CuCo_2S_4$, MXene/$CuCo_2S_4$), polytetrafluoroethyene (PTFE) and acetylene black with mass ratio of 8: 1: 1 were directly loaded on Ni foam and used as a working electrode. The loading mass of the active materials was weighted to be approximately 3.5 mg cm^{-2}. All electrochemical tests were carried out on a CHI660E electrochemical workstation

with the Ni foam carrying active material as the working electrode, Pt wire as the counter electrode was, and AgCl/Ag as the reference electrode. Besides, the electrolysis was 6 M KOH aqueous solution (50 mL). The galvanostatic charge/discharge (GCD) test and cycling test were conducted using a LAND battery program-control test system (CT2001A).

Fabrication of asymmetric supercapacitor device

The asymmetric supercapacitor (ASC) was fabricated by using Ti_3C_2 MXene/$CuCo_2S_4$ nanohybrid as the positive electrode, an activated carbon as the negative electrode and the electrospun PVdF membrane containing 6 M KOH as the separator as well as electrolyte. Based on the charge balance equation ($q^+=q^-$), the optimal mass ratio of both electrodes is found to be 0.7. Hence, the mass loading of Ti_3C_2 MXene/$CuCo_2S_4$ and activated carbon is about 3.5 and 5 mg cm^{-2}, respectively. The cyclic voltammetry and galvanostatic charge-discharge studies were performed for Ti_3C_2 MXene/$CuCo_2S_4$//AC based ASC and the specific capacitance, energy and power densities were calculated based on the mass of cathode and anode materials.

The specific capacity C_s (C g^{-1}) of $CuCo_2S_4$, MXene and MXene/$CuCo_2S_4$ electrodes is obtained from Equation (S1).[1]

$$C_s = I\Delta t/m \qquad \text{(S1)}$$

where Δt (s) is the discharge time, I (A) is the applied current, m (g) is the is the loading mass of active material.

The specific capacity C_{device} (C g^{-1}), specific energy E (Wh kg^{-1}) and specific power P (W kg^{-1}) of asymmetric supercapacitors can be calculated from the Equation (S2-S4), respectively. [1-3]

$$C_{device} = I\Delta t/m \qquad \text{(S2)}$$

$$E = \frac{\int_{t1}^{t2} IV_{(t)}dt}{m \times 3.6} \qquad \text{(S3)}$$

$$P = 3600E/\Delta t \qquad \text{(S4)}$$

where I (A) corresponds to the applied current, Δt (s) means the discharging time, m

(g) represents the total loading mass of active materials on both cathode and anode, t_1 (s) is the initial time after IR drop, t_2 (s) is the final time of discharge, and $\int V(t)dt$ is the integrated area of discharge curves after IR drop.

The discharge profile is governed by the voltage polynomial expressed as:

$$V = V_o - mt^{0.5} \quad \text{(S5)}$$

where m is a diffusion parameter and is related to V_o, the initial applied maximum voltage and t is the time duration of the self-discharge process.

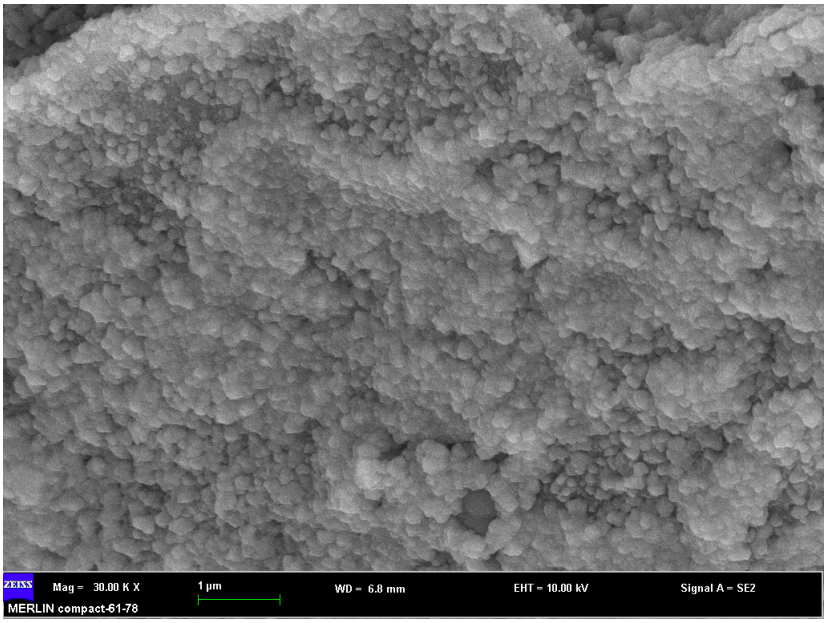

Fig. S1. SEM image for the single-phase $CuCo_2S_4$ nanoparticles.

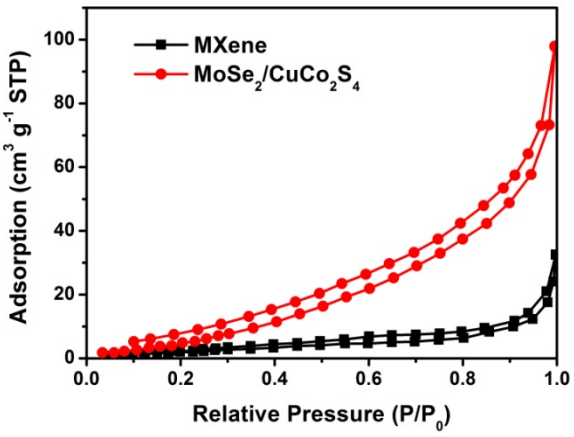

Fig. S2. The nitrogen adsorption-desorption isotherms of MXene and MXene/$CuCo_2S_4$.

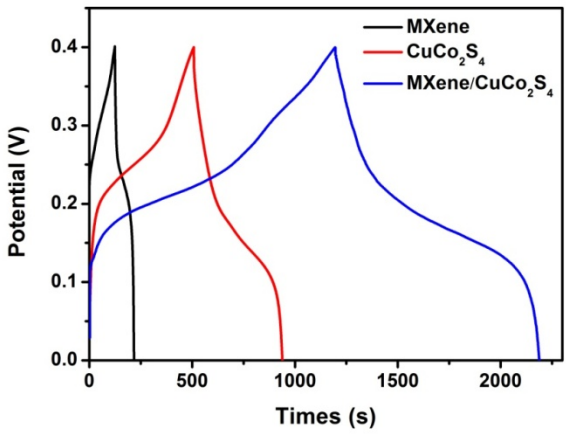

Fig. S3. Galvanostatic charge-discharge curves of MXene, $CuCo_2S_4$ and MXene/$CuCo_2S_4$ at a current density of 1 A g^{-1}.

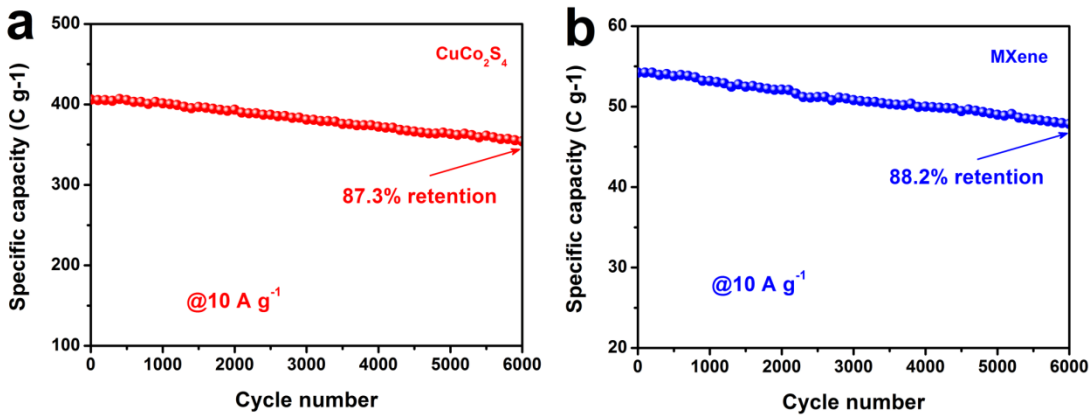

Fig. S4. Cycling performance of $CuCo_2S_4$ electrode (a) and MXene electrode (b) at 10 A g^{-1}.

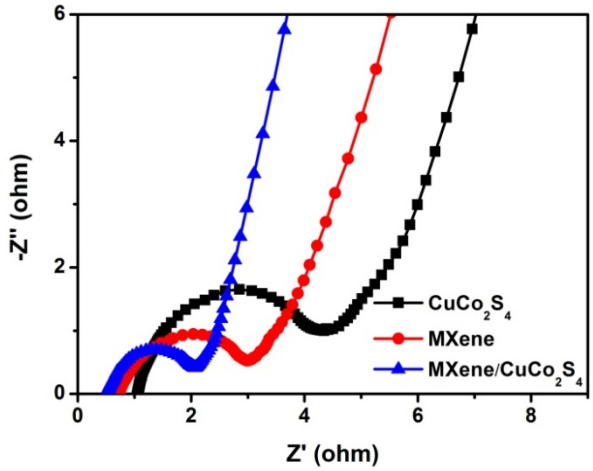

Fig. S5. The expanded high frequency region in fig. 4f.

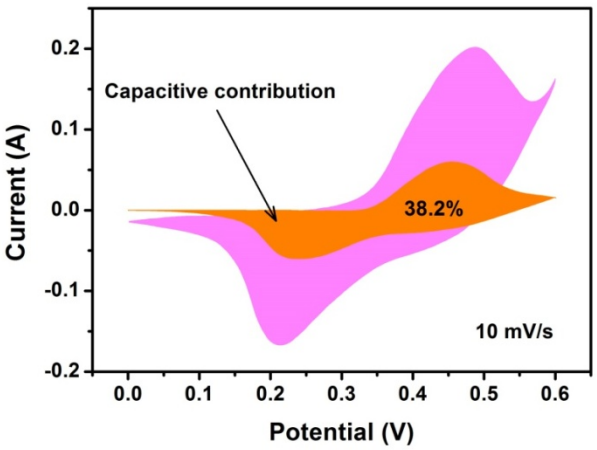

Fig. S6. Capacitance-dominated and diffusion-controlled contribution to charge storage of MXene/$CuCo_2S_4$ at a scan of 10 mV s^{-1}.

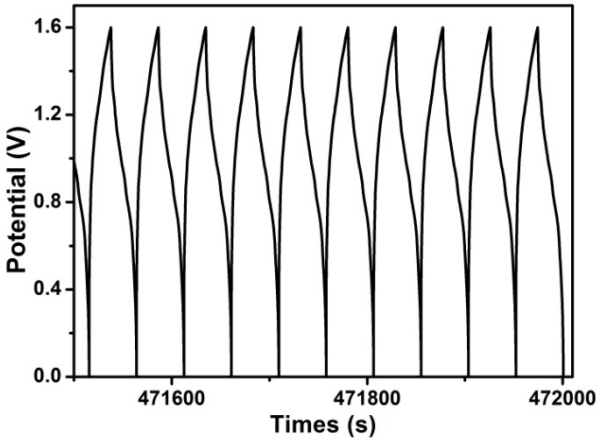

Fig. S7. The last 10 circles GCD curves of the hybrid supercapacitor device.

Table S1. Comparison of electrochemical performance of MXene/$CuCo_2S_4$ electrode with previous reports.

Materials	Electrolyte	Specific capacitance ($C\ g^{-1}$)	Cycling performance	Ref.
$Co(OH)_2/Ni_2Mn_1O_x$/NF	2 M KOH	949.02 at 1 A g^{-1}	83% after 5000 cycles at 10 A g^{-1}	[4]
CoNiFe LDH	1 M KOH	360 at 0.4 A g^{-1}	81.4% after 2000 cycles at 10 A g^{-1}	[5]
$CoNi_2Se_4$	6 M KOH	632.5 at 1 A g^{-1}	83.31% after 3000 cycles at 40 A g^{-1}	[6]
$Ni@NiMoO_4@Ni_3S_2$	6 M KOH	870 at 0.6 A g^{-1}	81.2% after 8000 cycles at 8 A g^{-1}	[7]
Co_3O_4	2 M KOH	576.8 at 1 A g^{-1}	82% after 5000 cycles at 5 A g^{-1}	[8]
$CoNi_2Se_4$	6 M KOH	602 at 1 A g^{-1}	98.3% after 5000 cycles at 40 A g^{-1}	[9]

Materials	Electrolyte	Specific capacitance ($C\ g^{-1}$)	Cycling performance	Ref.
Co_9S_8	3 M KOH	926 at 1 A g^{-1}	86% after 5000 cycles at 20 A g^{-1}	[10]
Fe_3O_4 nanoaggregates	3 M KOH	868.7 at 2 A g^{-1}	88.8% after 3000 cycles at 2 A g^{-1}	[11]
MnCoP	3 M KOH	879 at 2 A g^{-1}	94.4% after 6000 cycles at 6 mA cm^{-2}	[12]
(Ni,Mo)S_2/G	2 M KOH	951 at 1 A g^{-1}	—	[13]
MXene/$CuCo_2S_4$	6 M KOH	992.3 at 1 A g^{-1}	91.2% after 10000 cycles at 10 A g^{-1}	This work

References

[1] Wei, G.; Zhao, X.; Du, K.; Huang, Y.; An, C.; Qiu, S.; Liu, M.; Yao, S.; Wu, Y., Flexible asymmetric supercapacitors made of 3D porous hierarchical $CuCo_2O_4$@CQDs and Fe_2O_3@CQDs with enhancedperformance. Electrochim. Acta 2018, 283, 248-259.

[2] Vadiyar, M. M.; Liu, X.; Ye, Z., Highly porous silver dendrites on carbon nanotube wrapped copper cobaltite nano-flowers for boosting energy density and cycle stability of asymmetric supercapattery. J. Power Sources 2019, 415, 154-164.

[3] Shao, Y.; F., E.-K. M.; Sun, J.; Li, Y.; Zhang, Q.; Zhu, M.; Wang, H.; Dunn, B.; B., K. R., Design and mechanisms of asymmetric supercapacitors. Chem. Rev. 2018, 18, 9233-9280.

[4] H. Xuan, T. Liang, G. Zhang, Y. Guan, H. Li, R. Wang, P. Han, Y. Wu, Synthesis of hierarchical porous $Co(OH)_2/Ni_2Mn_1O_x$ composites on Ni foam for high performance battery-supercapacitor hybrid devices, Journal of Alloys and Compounds, 818 (2020) 153350.

[5] R. C. Rohit, A. D. Jagadale, S. K. Shinde, D. Y. Kim, V. S. Kumbhar, M. Nakayama, Hierarchical nanosheets of ternary CoNiFe layered double hydroxide for supercapacitors and oxygen evolution reaction, Journal of Alloys and Compounds, 863 (2021) 158081.

[6] J. A. Rajesh, Y. H. Lee, Y. H. Yun, V. H. V. Quy, S. H. Kang, H. Kim, K. S. Ahn, Potentiostatic deposition of $CoNi_2Se_4$ nanostructures on nickel foam as efficient battery-type electrodes for supercapacitors, Journal of Electroanalytical Chemistry, 850 (2019) 113371.

[7] L. Feng, P. Yang, W. Ling, S. Wang, J. Shi, F. Wang, 3D hierarchical flower-like $NiMoO_4$@ Ni_3S_2 composites on Ni foam for high-performance battery-type supercapacitors, Journal of Physics and Chemistry of Solids, 148 (2021) 109697.

[8] S. Kong, F. Yang, K. Cheng, T. Ouyang, K. Ye, G. Wang, D. Cao, In-situ growth of cobalt oxide nanoflakes from cobalt nanosheet on nickel foam for battery-type supercapacitors with high specific capacity, Journal of Electroanalytical Chemistry, 785 (2017) 103-108.

[9] J. A. Rajesh, Y. H. Lee, Y. H. Yun, V. H. V. Quy, S. H. Kang, H. Kim, K. S. Ahn, Bifunctional $NiCo_2Se_4$ and $CoNi_2Se_4$ nanostructures: Efficient electrodes for battery-type supercapacitors and electrocatalysts for the oxygen evolution reaction, Journal of Industrial and Engineering Chemistry, 79 (2019) 370-382.

[10] J. Li, Q. Li, J. Sun, Y. Ling, K. Tao, L. Han, Controlled Preparation of Hollow and Porous Co_9S_8 Microplate Arrays for High-Performance Hybrid Supercapacitors, Inorganic Chemistry, 59 (2020) 11174-11183.

[11] X. Li, Y. Xu, H. Wu, X. Qian, L. Chen, Y. Dan, Q. Yu, Porous Fe_3O_4/C nanoaggregates by

the carbon polyhedrons as templates derived from metal organic framework as battery-type materials for supercapacitors, Electrochimica Acta, 337 (2020) 135818.

[12] M. Amiri, S. E. Moosavifard, S. S. H. Davarani, S. K. Kaverlavani, M. Shamsipur, MnCoP hollow nanocubes as novel electrode material for asymmetric supercapacitors, Chemical Engineering Journal, 420 (2021) 129910.

[13] X. Yang, J. Mao, H. Niu, Q. Wang, K. Zhu, K. Ye, G. Wang, D. Cao, J. Yan, NiS_2/MoS_2 mixed phases with abundant active edge sites induced by sulfidation and graphene introduction towards high-rate supercapacitors, Chemical Engineering Journal, 406 (2021) 126713.